Interpreting the GeV and TeV pulsar emission

Constantinos Kalapotharakos

NASA/Goddard Space Flight Center,

University of Maryland, College Park

Collaborators

Alice Harding (NASA GSFC, Los Alamos National Laboratory)

Demos Kazanas (NASA GSFC)

Zorawar Wadiasingh (NASA GSFC)

Christo Venter (North-West University, South Africa)

Monica Barnard(University of Johannesburg, South Africa)

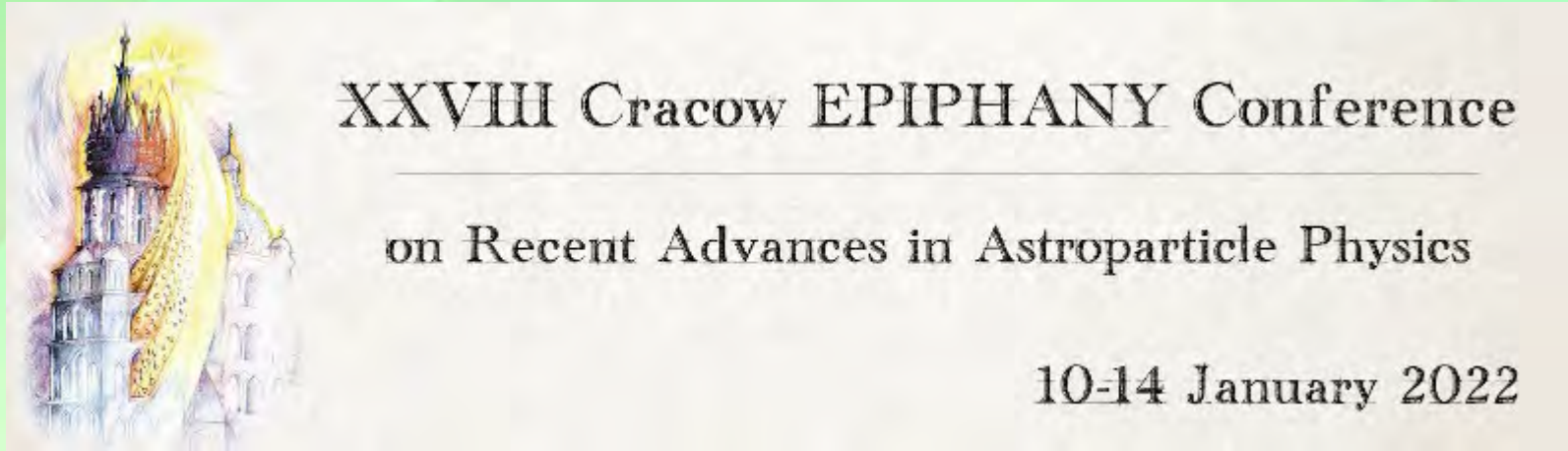

Outline

- Fermi era (GeV), VHE (up to multi TeV) pulsed detections
- Fundamental plane of γ-ray pulsars
- Kinetic PIC global magnetosphere models
  Separatrix injection model
  Broad-spectrum phenomenology (γ-ray light curves & the FP)
- Broadband & VHE emission models
- Summary

(MeV era, AMEGO?)

FERMI

Fermi revolutionized the study of γ-ray pulsars playing a catalytic role on the modeling of the high-energy emission in pulsar magnetospheres.

$N_p \longrightarrow \times 45 \quad N_p > 270$ (117 in 2PC; Abdo et al. 2013)

Discovery ⟶ Astronomy

established a number of trends and correlations

Observed γ-ray emission originates in the outer magnetoshpere

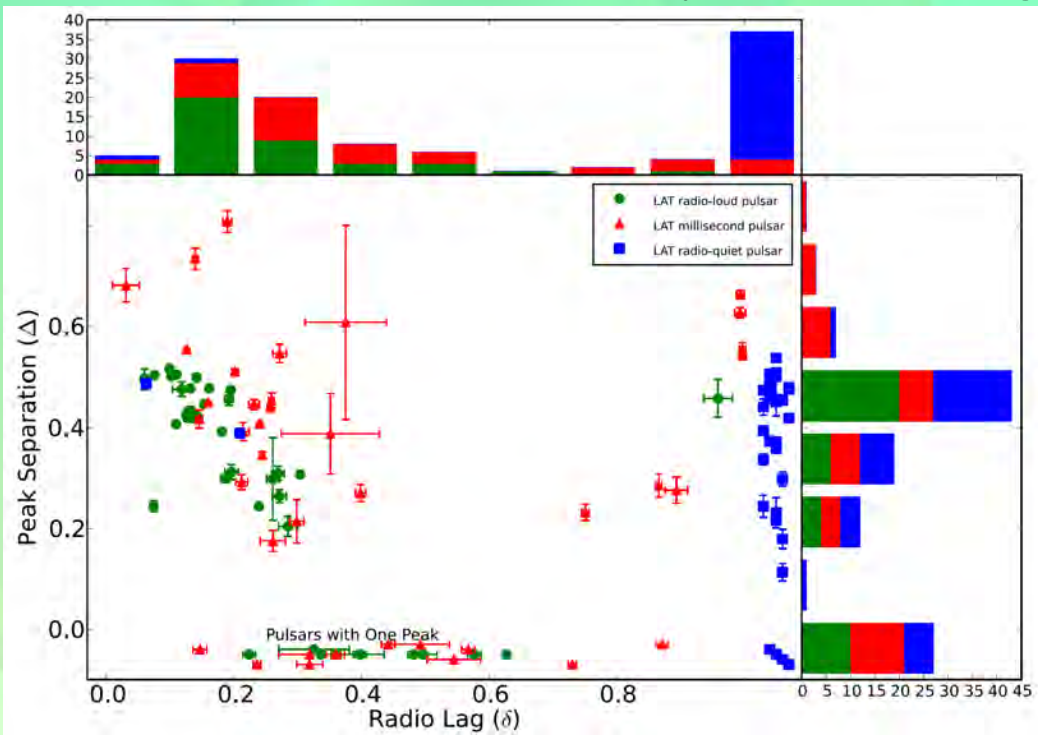

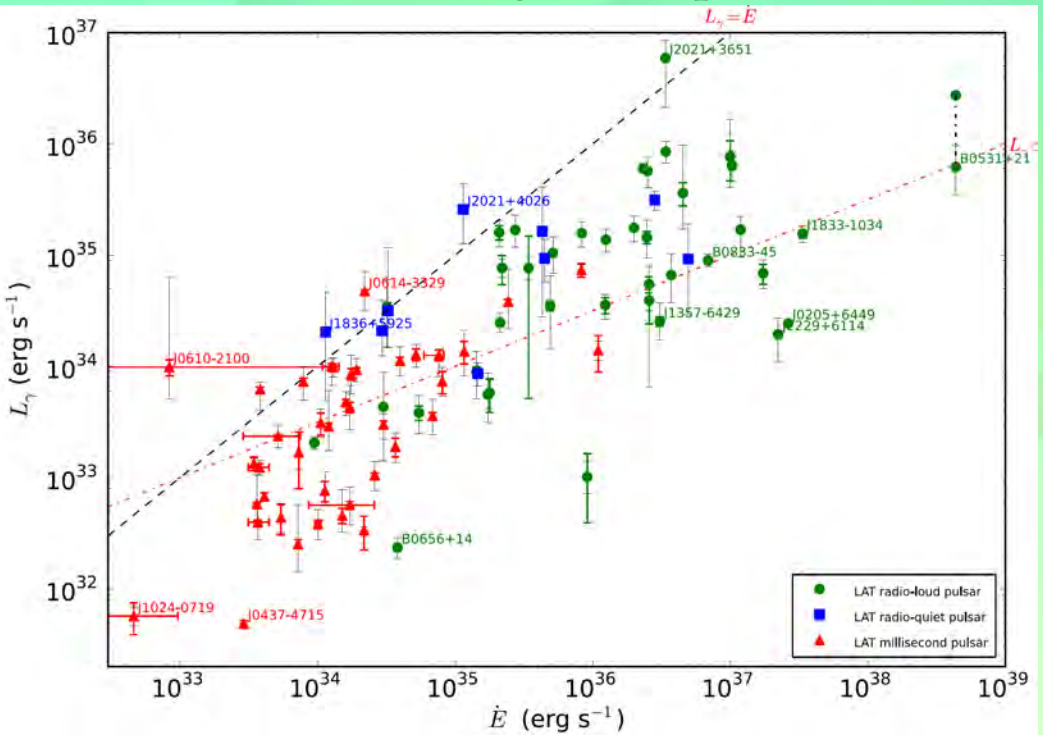

VHE pulsed detections

Recent detections by *MAGIC* and *HESSII* of very high energy (VHE) emission from the **Crab** (Ansoldi et al. 2016), **Vela** (Djannati-Atai et al. 2017), and **Geminga** (Acciari et al. 2020) pulsars imply an additional emission component, and inverse Compton (IC) seems to be the most reasonable candidate (Rudak & Dyks 2017, Harding et al. 2018, Harding et al. 2021).

Crab pulsar

Detection up to 1.5 TeV

MAGIC 40 GeV – 1 TeV (Ansoldi et al. 2016)

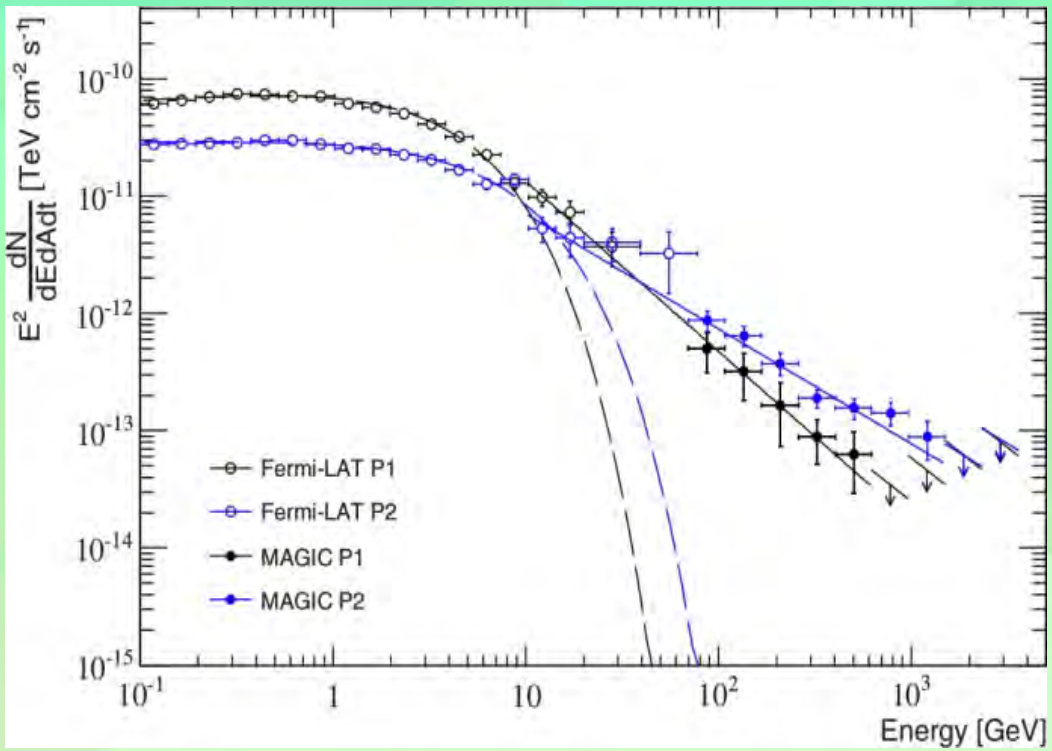

In phase with the *Fermi* peaks

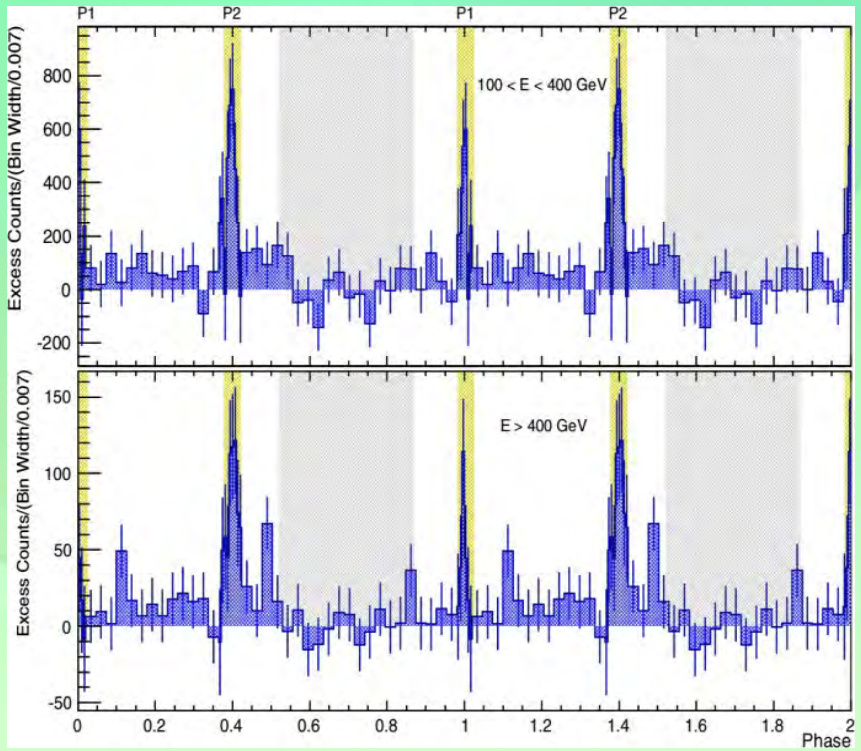

VHE pulsed detections

Recent detections by *MAGIC* and *HESSII* of very high energy (VHE) emission from the **Crab** (Ansoldi et al. 2016), **Vela** (Djannati-Atai et al. 2017), and **Geminga** (Acciari et al. 2020) pulsars imply an additional emission component, and inverse Compton (IC) seems to be the most reasonable candidate (Rudak & Dyks 2017, Harding et al. 2018, Harding et al. 2021).

Vela pulsar

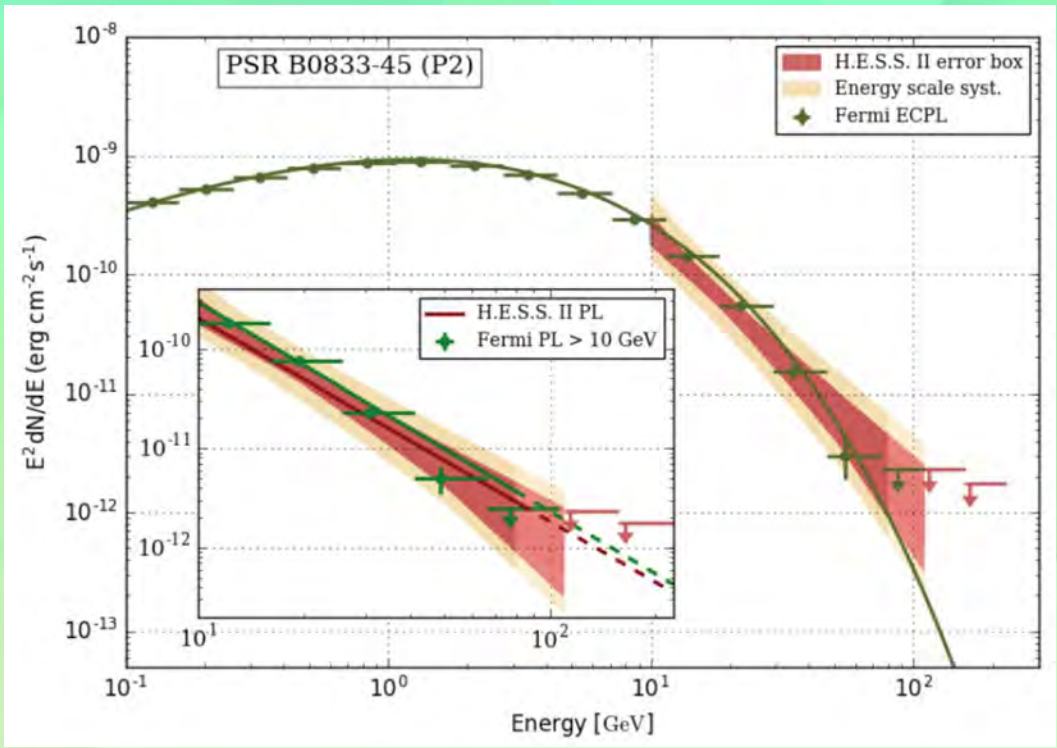

Detection up to 3-(>7 TeV)

(Djannati-Atai 2018)

Only 2nd peak is detected

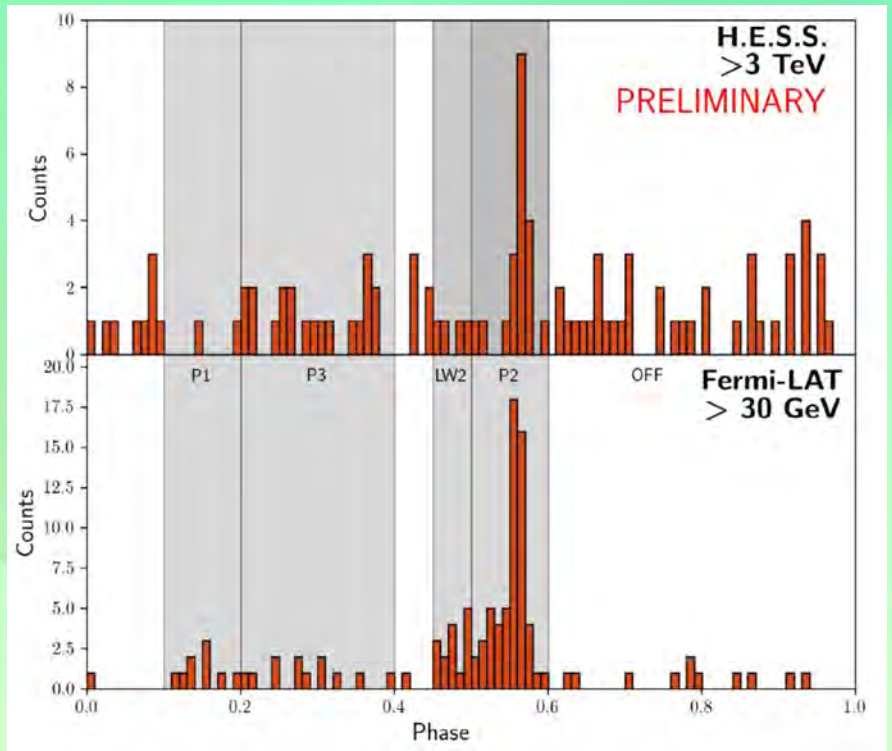

FFE field structure

Kalapotharakos et al. (2012)

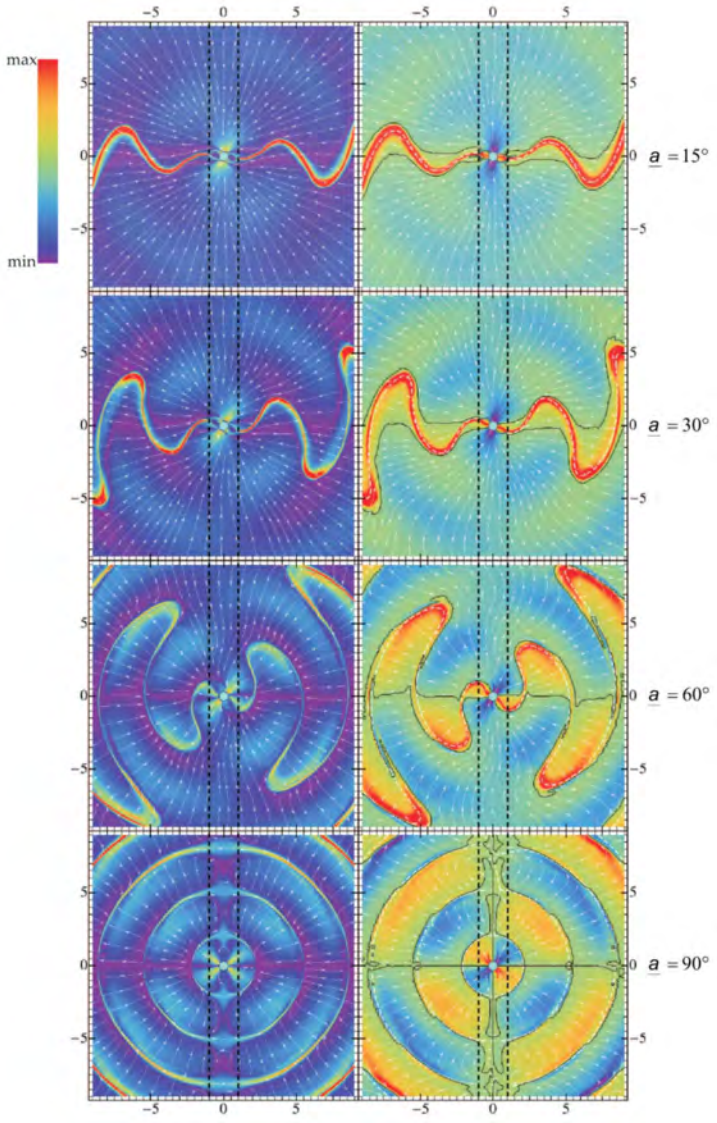

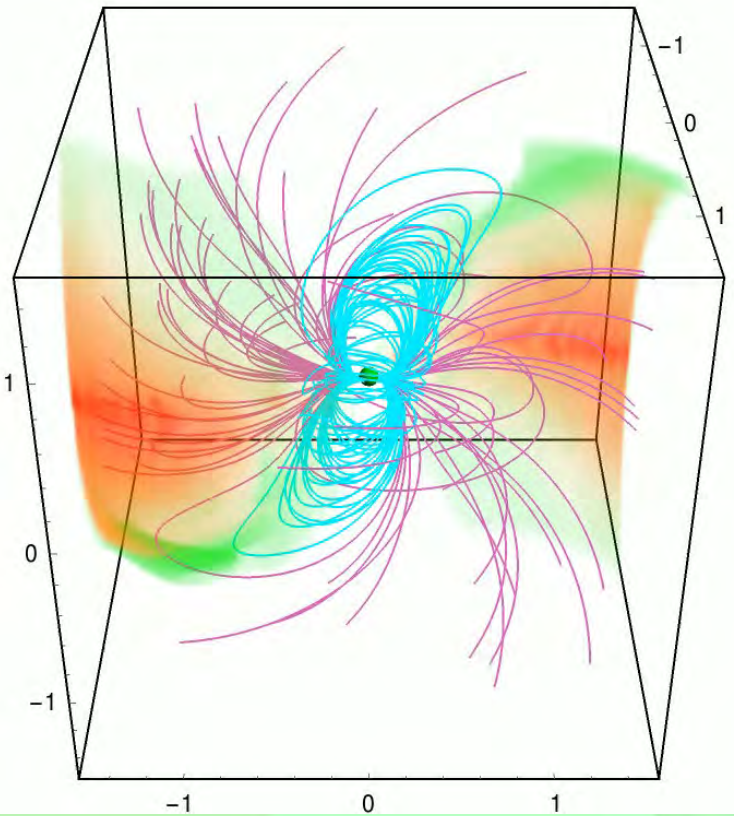

Bai & Spitkovsky 2010, Contopoulos & Kalapotharakos 2010, Kalapotharakos et al. (2014, 2017, 2018, 2019), Uzdensky & Spitkovsky 2014, Brambilla et al. (2015, 2018), Cerruti et al. 2016, Philippov & Spitkovsky 2018, Hakobyan et al. 2019

Bogovalov (1999)

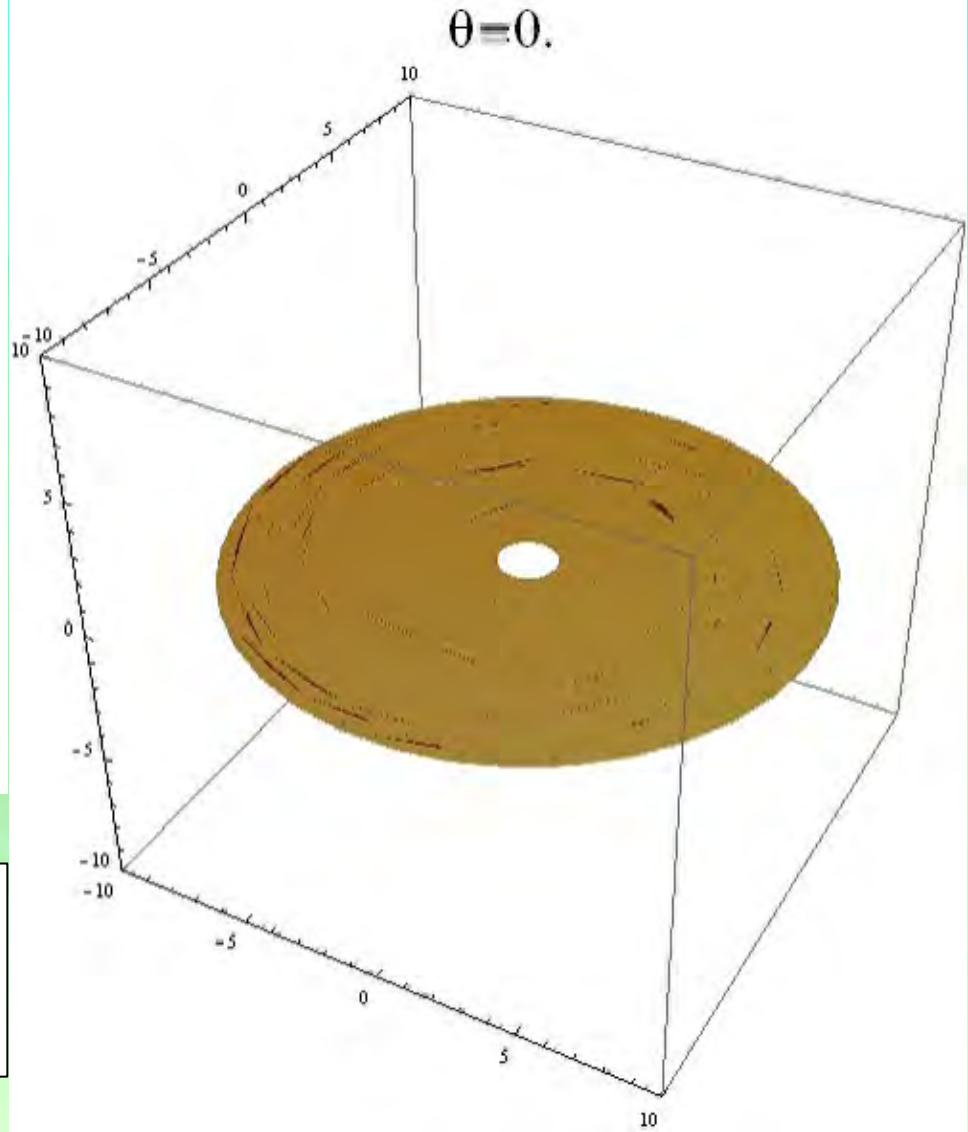

Fundamental Plane (Theory)

Assumptions

1) Radiation Reaction Limit Regime

2) At the ECS near the LC

CR

Kalapotharakos et al. (2019)

$R_C \propto R_{LC} \propto P$

$B_{LC} \propto B_* R_{LC}^{-3} \propto B_* P^{-3}$

$\gamma_L \propto \epsilon_{cut}^{1/3} P^{1/3}$

$E_{BLC} B_{LC} \propto \gamma_L^4 R_C^{-2}$

$E_{BLC} \propto \epsilon_{cut}^{4/3} P^{7/3} B_*^{-1}$

$L_{\gamma 1} \propto \epsilon_{cut}^{4/3} P^{-2/3}$

$\rho_{GJ} \propto B_* P^{-1}$

$\dot{\mathcal{E}} \propto B_*^2 P^{-4}$

$$L_\gamma \propto \epsilon_{cut}^{4/3} B_*^{1/6} \dot{\mathcal{E}}^{5/12}$$

$$\frac{2 q_e^2 \gamma_L^4}{3 m_e c \, R_C(\theta)} = \frac{q_e \mathbf{v} \cdot \mathbf{E}}{m_e c^2}$$

$$\epsilon_{cut} = \frac{3}{2} c \hbar \frac{\gamma_L^3}{R_C(\theta)}$$

Fundamental Plane (Theory)

Assumptions

1) Radiation Reaction Limit Regime

2) At the ECS near the LC

Kalapotharakos et al. (2019)

$R_C \propto R_{LC} \propto P$

$E_{BLC} B_{LC} \propto \gamma_L^4 R_C^{-2}$

$\rho_{GJ} \propto B_* P^{-1}$

$\dot{\mathcal{E}} \propto B_*^2 P^{-4}$

$B_{LC} \propto B_* R_{LC}^{-3} \propto B_* P^{-3}$

$E_{BLC} \propto \epsilon_{cut}^{4/3} P^{7/3} B_*^{-1}$

$\gamma_L \propto \epsilon_{cut}^{1/3} P^{1/3}$

$L_{\gamma 1} \propto \epsilon_{cut}^{4/3} P^{-2/3}$

CR

$$L_\gamma \propto \epsilon_{cut}^{4/3} B_*^{1/6} \dot{\mathcal{E}}^{5/12}$$

$R_C \propto r_g \propto \gamma_L B_*^{-1} P^3$

$$L_\gamma \propto \epsilon_{cut} \dot{\mathcal{E}}$$

SR

Fundamental Plane (Observations)

88 Fermi YPs+MPs

$$L_{\gamma(3D)} = 10^{14.2\pm2.3}\,\epsilon_{cut}^{1.18\pm0.24}\,B_*^{0.17\pm0.05}\,\dot{\mathcal{E}}^{0.41\pm0.08}$$

$\epsilon_{cut}(\mathrm{MeV}), B_*(\mathrm{G}), L_\gamma, \dot{\mathcal{E}}(\mathrm{erg/s})$

Fermi data

Kalapotharakos et al. (2019)

$$L_\gamma \propto \epsilon_{cut}^{4/3}\,B_*^{1/6}\,\dot{\mathcal{E}}^{5/12}$$

Theory CR

Fundamental Plane (Observations)

88 Fermi YPs+MPs

$$L_{\gamma(3D)} = 10^{14.2\pm2.3}\,\epsilon_{cut}^{1.18\pm0.24}\,B_*^{0.17\pm0.05}\,\dot{\mathcal{E}}^{0.41\pm0.08}$$

Fermi data

$\epsilon_{cut}(\mathrm{MeV}), B_*(\mathrm{G}), L_\gamma, \dot{\mathcal{E}}(\mathrm{erg/s})$

Kalapotharakos et al. (2019)

$$L_\gamma \propto \epsilon_{cut}^{4/3}\,B_*^{1/6}\,\dot{\mathcal{E}}^{5/12}$$

Theory CR

Fundamental Plane (Observations)

88 Fermi YPs+MPs

$$L_{\gamma(3D)} = 10^{14.2\pm2.3}\,\epsilon_{cut}^{1.18\pm0.24}\,B_*^{0.17\pm0.05}\,\dot{\mathcal{E}}^{0.41\pm0.08}$$

$\epsilon_{cut}(\mathrm{MeV}), B_*(\mathrm{G}), L_\gamma, \dot{\mathcal{E}}(\mathrm{erg/s})$

Fermi data

Kalapotharakos et al. (2019)

$$L_\gamma \propto \epsilon_{cut}^{4/3}\,B_*^{1/6}\,\dot{\mathcal{E}}^{5/12}$$

Theory CR

Ploeg et al. (2020), independently confirmed these results working on the population of MSPs

$$L_{\gamma(3D)} \propto \epsilon_{cut}^{1.2\pm0.3}\,B_*^{0.1\pm0.4}\,\dot{\mathcal{E}}^{0.5\pm0.1}$$

Fundamental Plane (Observations)

4D-space is hard to visualize

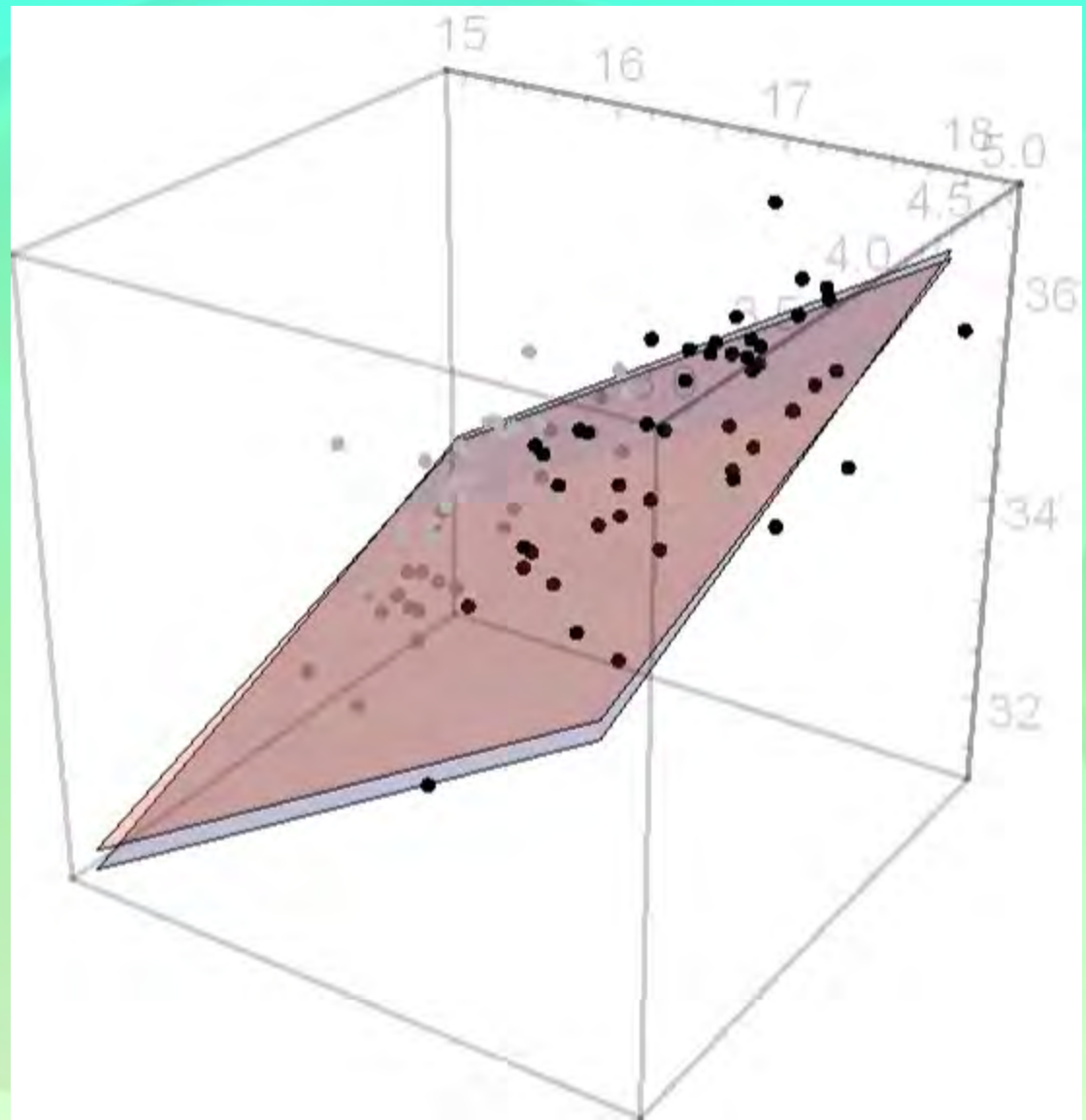

$$x = B_*^{1/6} \dot{\mathcal{E}}^{5/12}$$
$$y = \epsilon_{cut}^{4/3}$$
$$z = L_\gamma$$

$z \propto x\, y$
(Theory)

$z \propto x^{0.99}\, y^{0.88}$
(Fermi data)

- Fermi YP
- Fermi MP

Fundamental Plane (Observations)

4D-space is hard to visualize

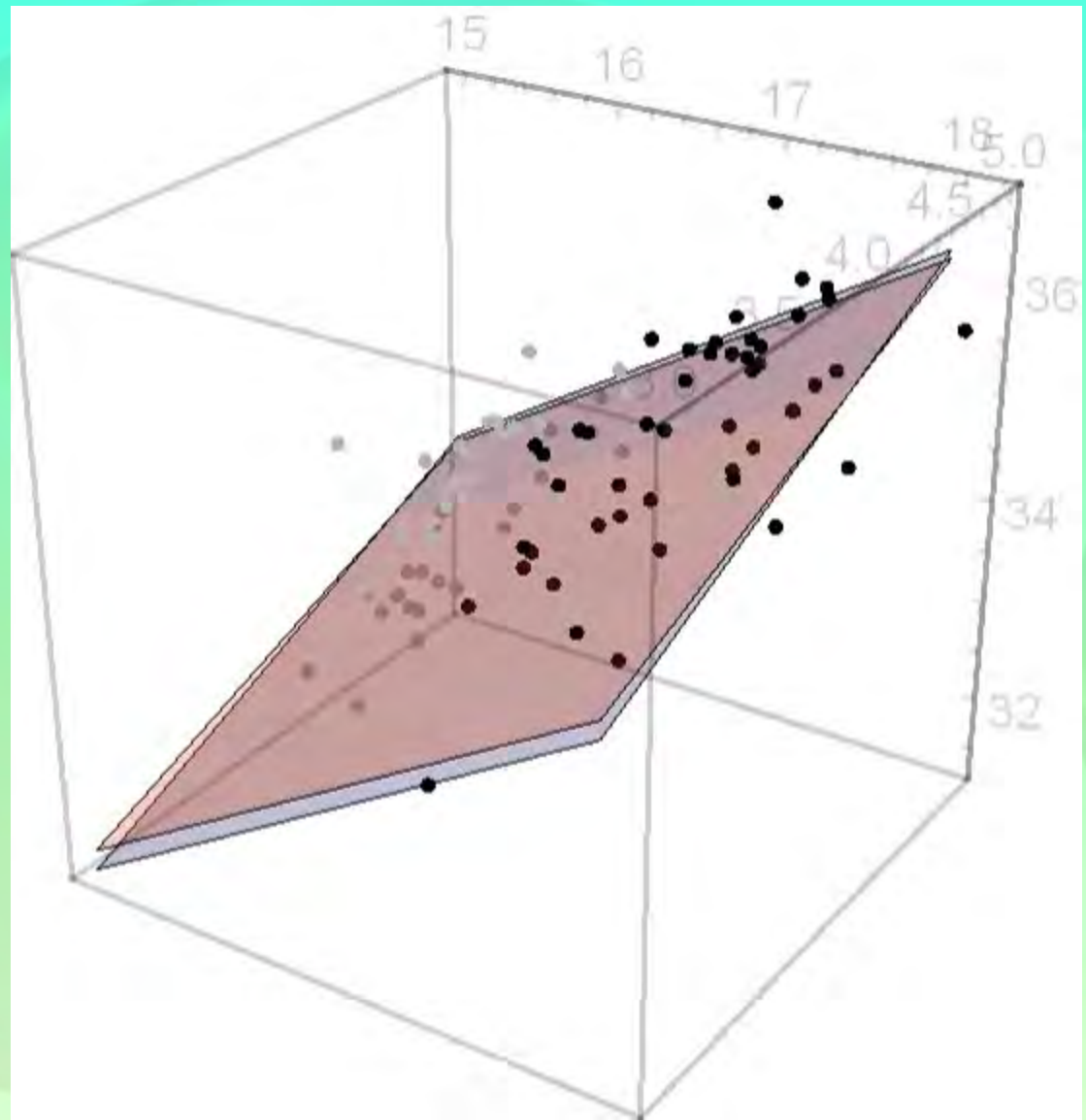

$$x = B_*^{1/6} \dot{\mathcal{E}}^{5/12}$$
$$y = \epsilon_{cut}^{4/3}$$
$$z = L_\gamma$$

$z \propto x\, y$
(Theory)

$z \propto x^{0.99}\, y^{0.88}$
(Fermi data)

- Fermi YP
- Fermi MP

Fundamental Plane (Observations)

4D-space is hard to visualize

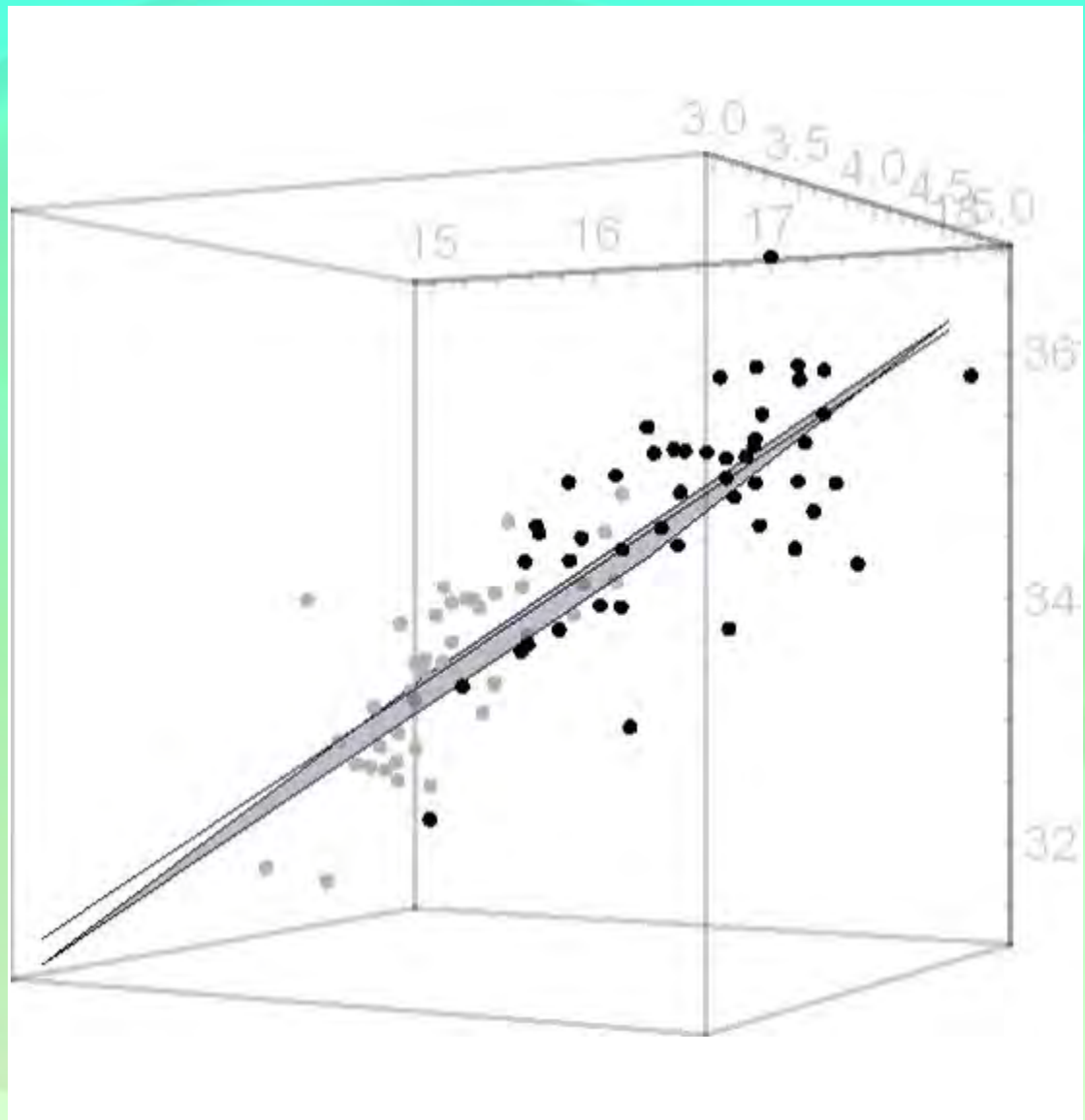

$$x = B_*^{1/6} \dot{\mathcal{E}}^{5/12}$$
$$y = \epsilon_{cut}^{4/3}$$
$$z = L_\gamma$$

$z \propto x\, y$
(Theory)

$z \propto x^{0.99}\, y^{0.88}$
(Fermi data)

- Fermi YP
- Fermi MP

Fundamental Plane (Observations)

4D-space is hard to visualize

$$x = B_*^{1/6}\dot{\mathcal{E}}^{5/12}$$
$$y = \epsilon_{cut}^{4/3}$$
$$z = L_\gamma$$

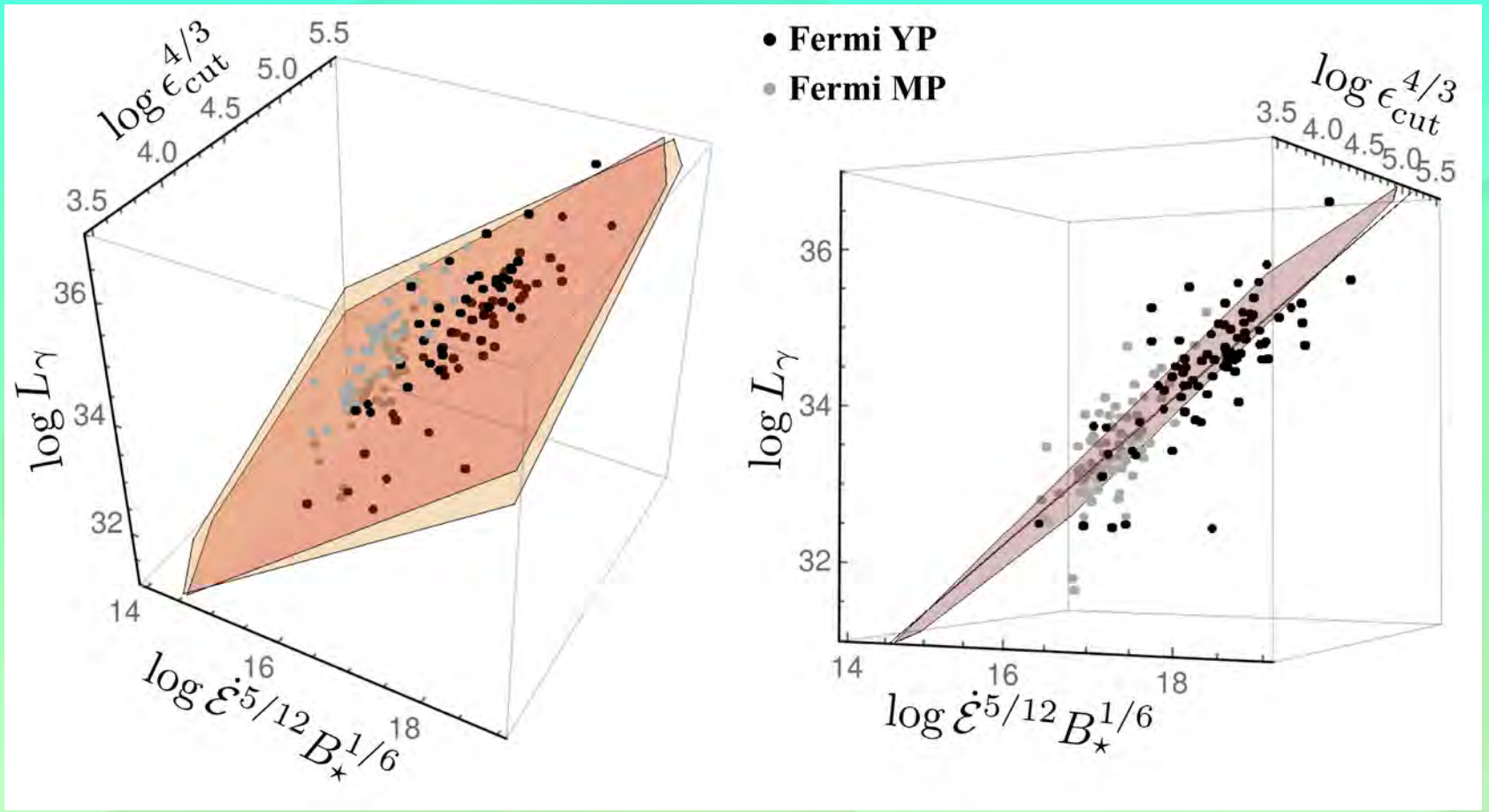

$$L_\gamma \propto \epsilon_{\rm cut}^{1.49\pm0.24} B_\star^{0.13\pm0.03} \dot{\mathcal{E}}^{0.40\pm0.06}$$

Based on 4FGL data and spectral analysis 162 Pulsars (× 2)

Kalapotharakos et al. (in prep)

- Fermi YP
- Fermi MP

3D Kinetic Models (PIC)

Kinetic PIC simulations provide a path to self-consistency.

Field structure & particle distributions are consistent with each other

3D Particle-In-Cell code

Kalapotharakos et al. (2018)
Brambilla et al. (2018)
Kalapotharakos et al. (2022, in prep)

C-3PA

- Cartesian
- Conservative
- Vay's algorithm
- Current Smoothing
- Radiation Reaction Forces
- Load Balancing
- Field Line Dependent Particle Injection

Pleiades & Discover Supercomputers, NASA
$\sim$ 4000cpus
$\sim 10^7 - 10^9$ particles

3D Kinetic Models (PIC)

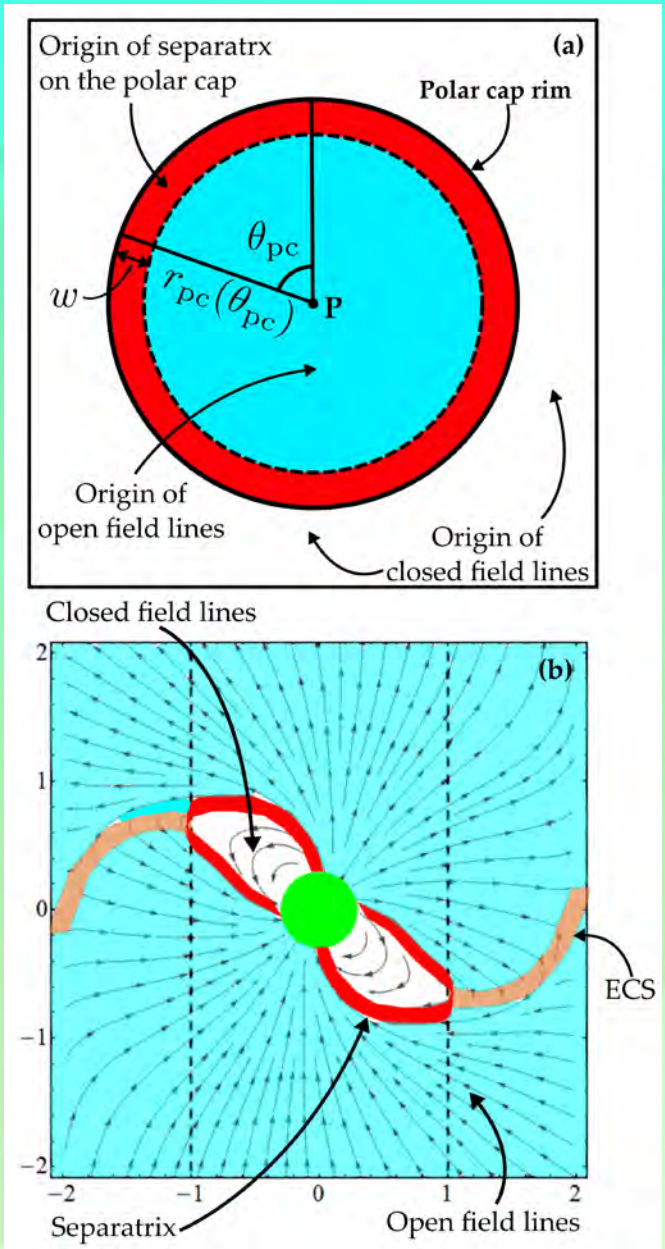

Separatrix injection model

The γ-ray pulsar radiation is mainly regulated by

1. **The particle injection rate $\mathcal{F}_s$ along the separatrix**
2. **The width w of the separatrix zone**

Kalapotharakos et al. (in prep)

Requirements

The particle injection rate along the open and the closed field-lines is <u>not very small</u>.

$(> 5\mathcal{F}_{GJ}^{0})$

However, it is <u>not necessary to be high</u>.

$(< 10\mathcal{F}_{GJ}^{0})$

3D Kinetic Models (PIC)

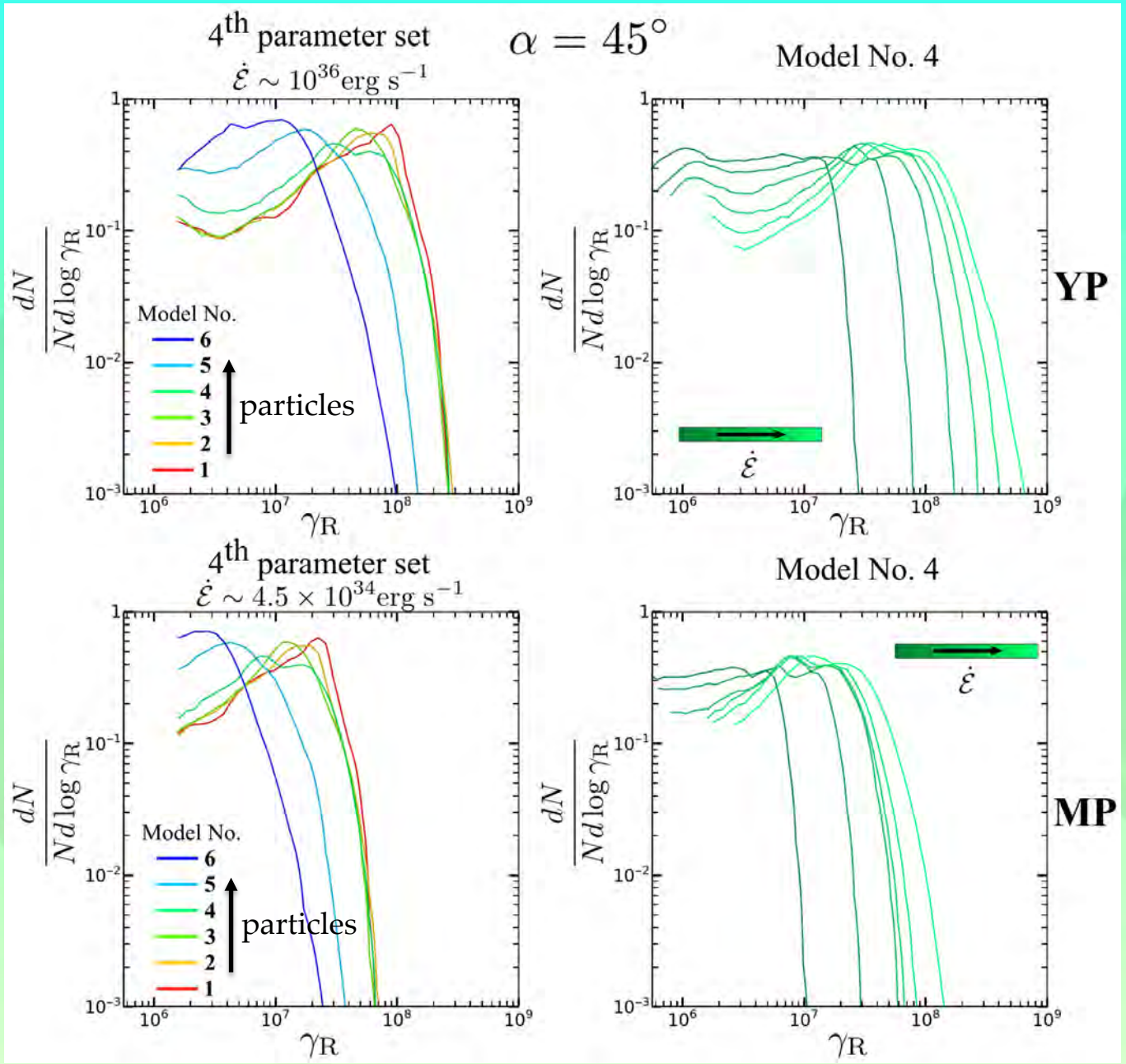

Important for the VHE and the ICS mechanism

↑ particles ↓ $E_{\rm acc}$ $\gamma_{\rm L}$

↑ $B_\star$ ↑ $E_{\rm acc}$

↑ Ω ↑ $\gamma_{\rm L}$

$\dot{\mathcal{E}} \propto B_*^2 P^{-4} \propto B_*^2 \Omega^4$

Kalapotharakos et al. (2018, 2022 in prep)

3D Kinetic Models (PIC)

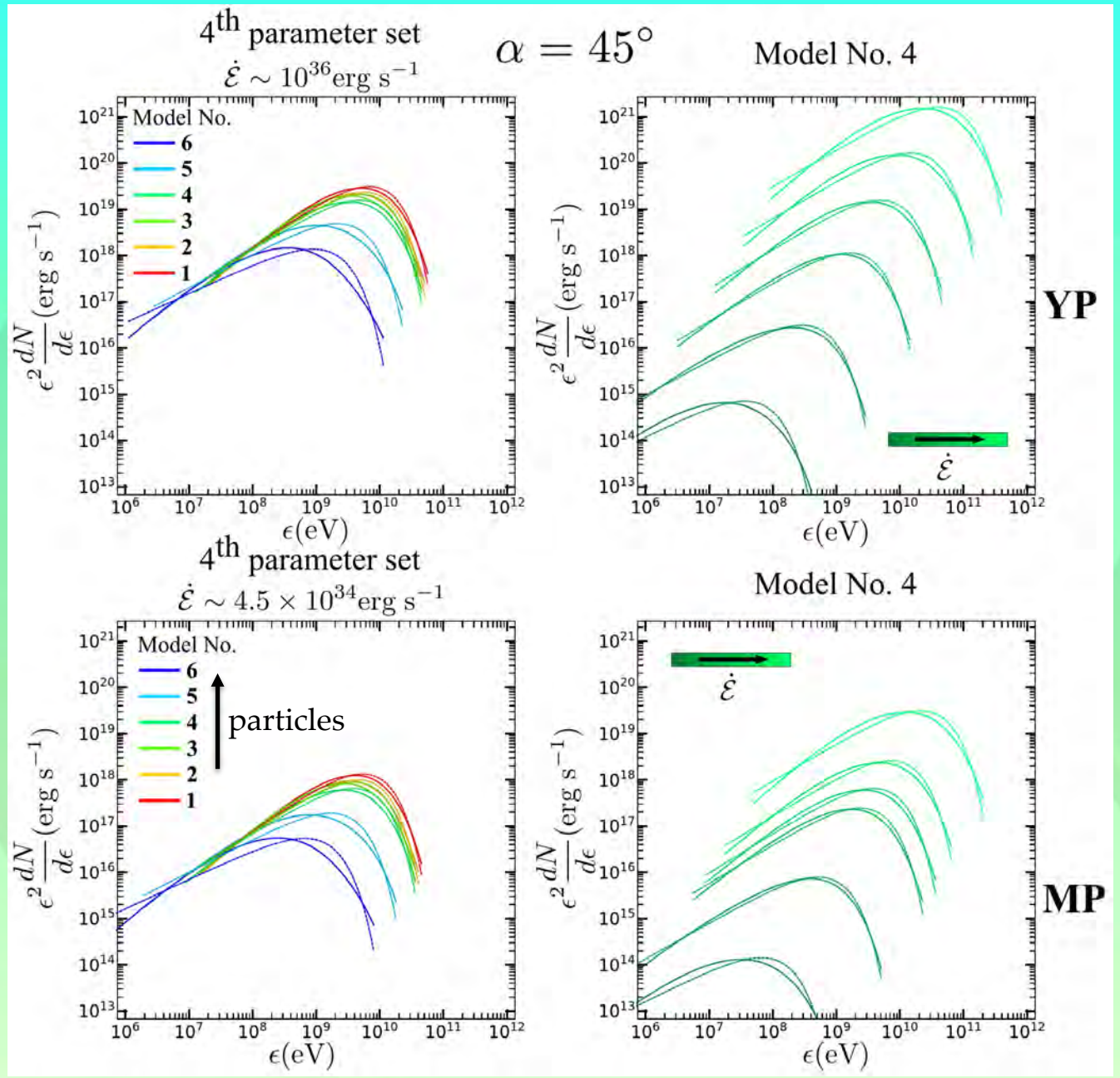

particles ↑ → $E_{\rm acc}$ ↓, $\gamma_{\rm L}$ ↓, $\epsilon_{\rm cut}$ ↓

$B_\star$ ↑, Ω ↑ → $E_{\rm acc}$ ↑, $\gamma_{\rm L}$ ↑, $\epsilon_{\rm cut}$ ↑

$$\dot{\mathcal{E}} \propto B_*^2 P^{-4} \propto B_*^2 \Omega^4$$

Kalapotharakos et al. (2018, 2022 in prep)

Fundamental Plane Observations & PIC Models

$L_\gamma \propto \epsilon_{cut}^{1.18\pm0.24} B_*^{0.17\pm0.05} \dot{\mathcal{E}}^{0.41\pm0.08}$ **Fermi data**

$L_\gamma \propto \epsilon_{cut}^{4/3} B_*^{1/6} \dot{\mathcal{E}}^{5/12}$ **Theory CR**

$L_\gamma \propto \epsilon_{cut}^{1.39\pm0.06} B_*^{0.17\pm0.02} \dot{\mathcal{E}}^{0.41\pm0.04}$ **PIC Models**

Fundamental Plane Observations & PIC Models

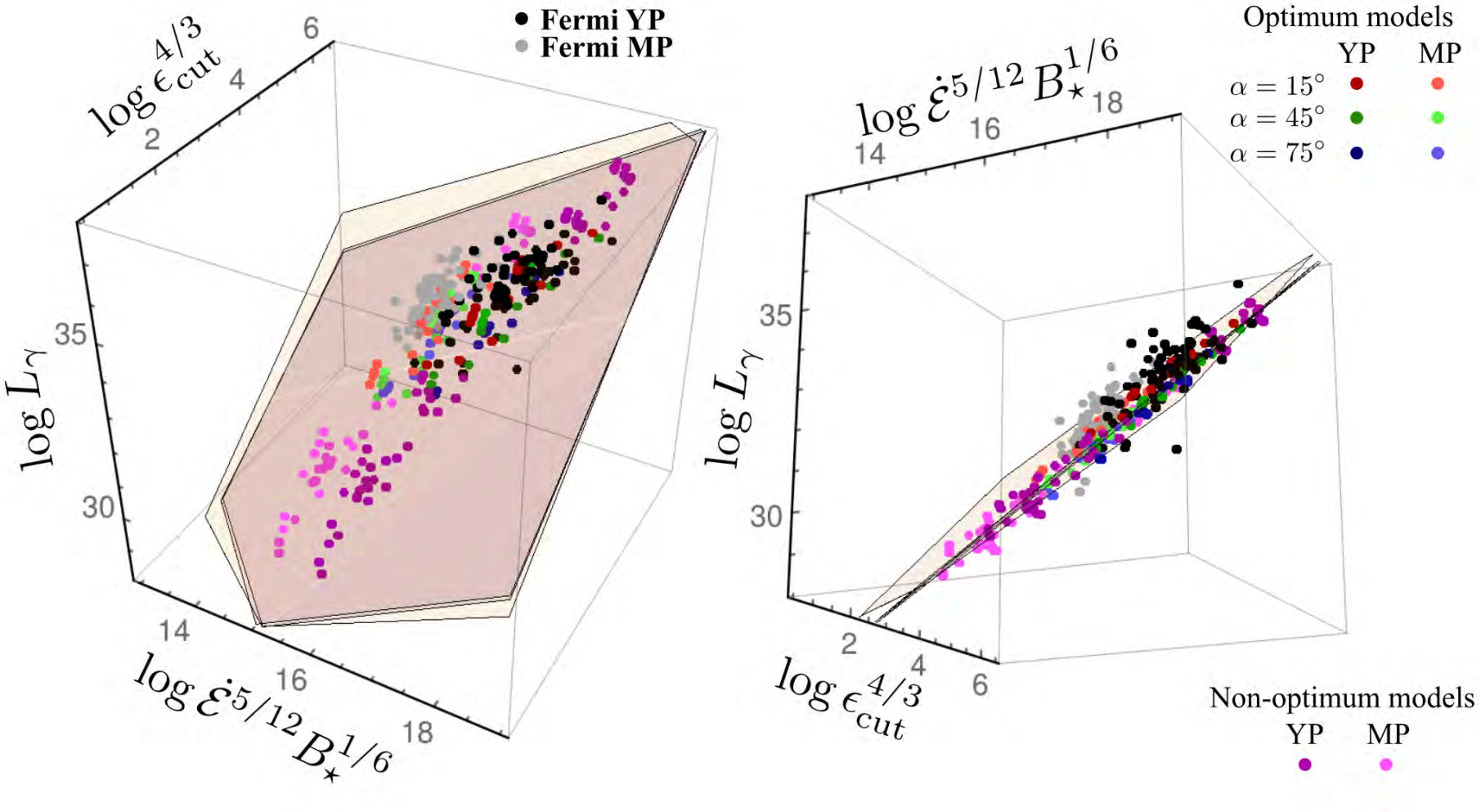

- Fermi YP
- Fermi MP

Colored points: PIC models

Kalapotharakos et al. (2022 in prep)

Fundamental Plane Observations & PIC Models

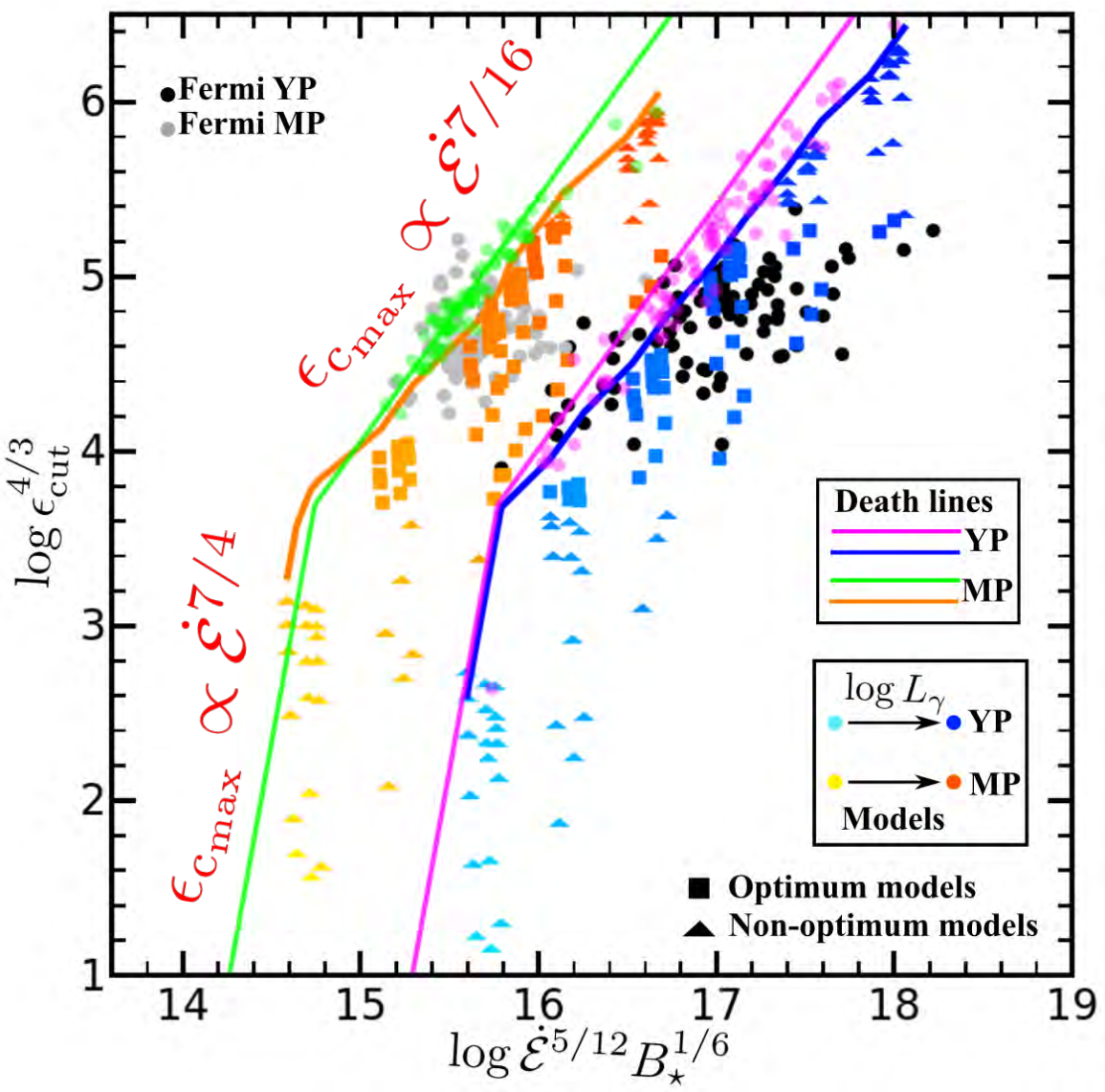

Death lines and death valleys

MeV pulsars era?

AMEGO, e-ASTROGAM, GECCO, and COSI

$$E_{\rm acc} \sim B_{\rm LC} \longrightarrow \gamma_{\rm RRL} \leq \gamma_{\rm max} \sim \gamma_{\rm pc}$$

Kalapotharakos et al. (2022 in prep)

Fundamental Plane Observations & PIC Models

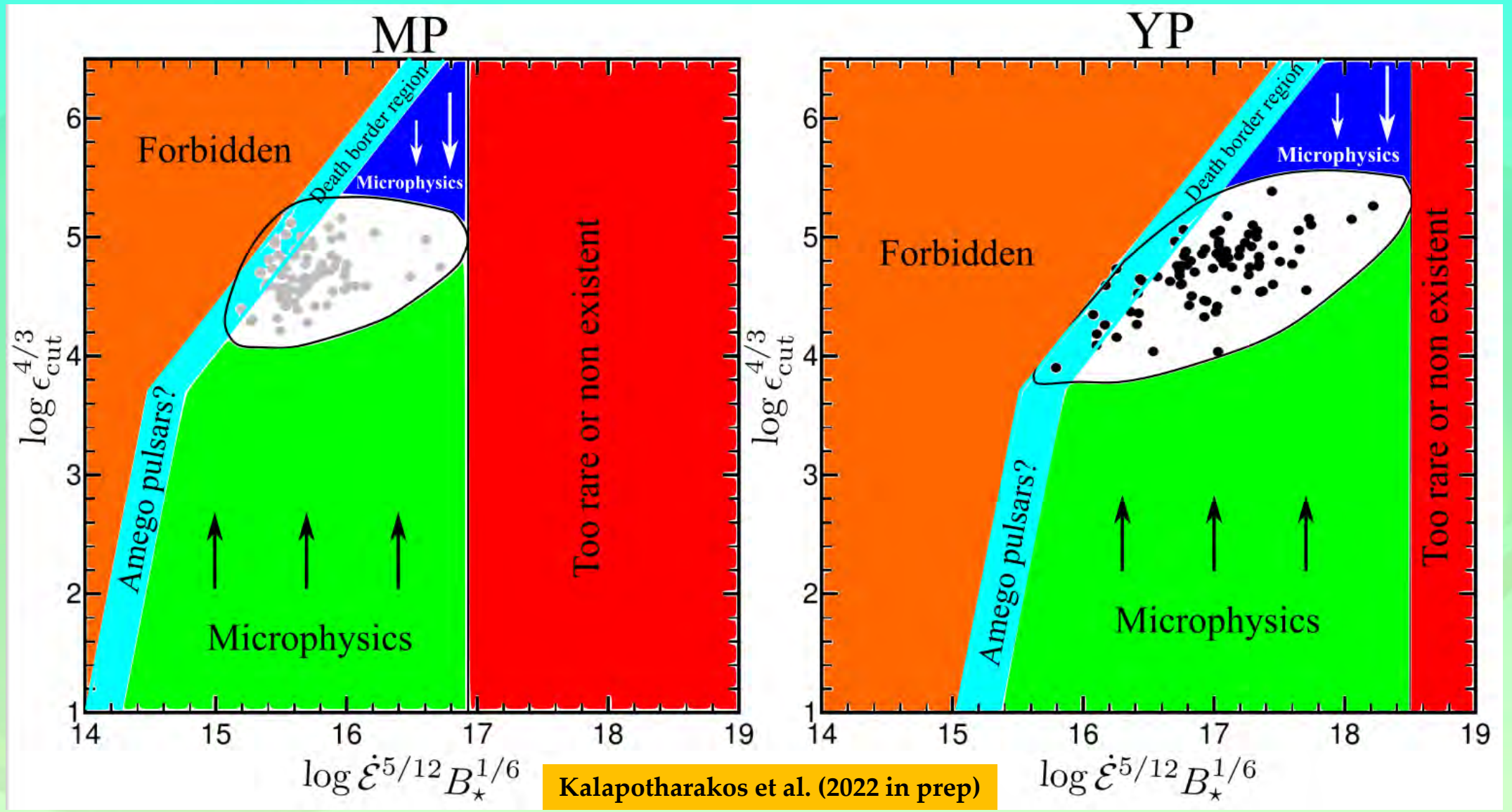

Kalapotharakos et al. (2022 in prep)

VHE pulsed emission (TeV+)

5+2 parameters: $E_{||}^{\text{low}}$, $E_{||}^{\text{high}}$, M_+, r_{radio}, J/J_{GJ} + α, ζ

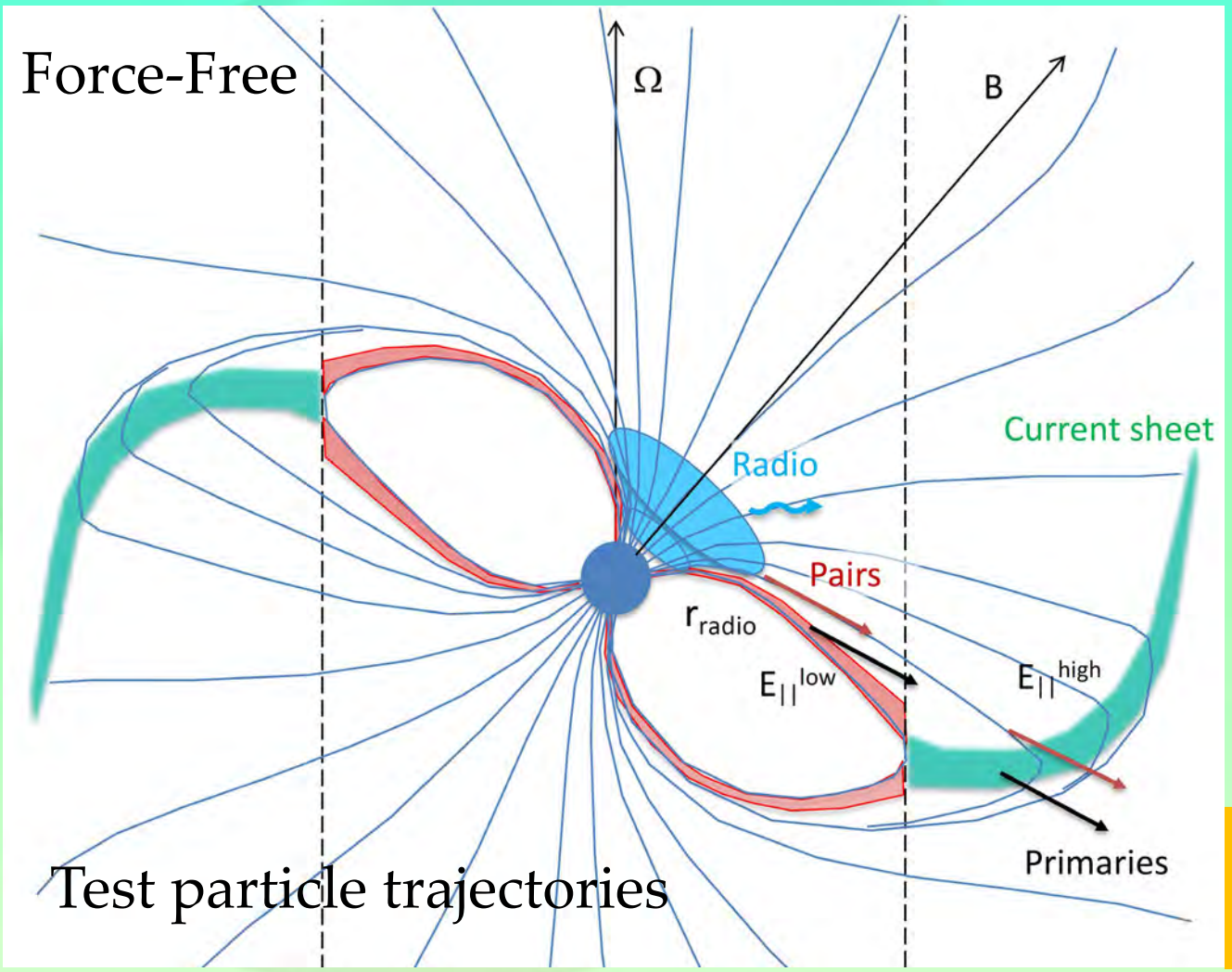

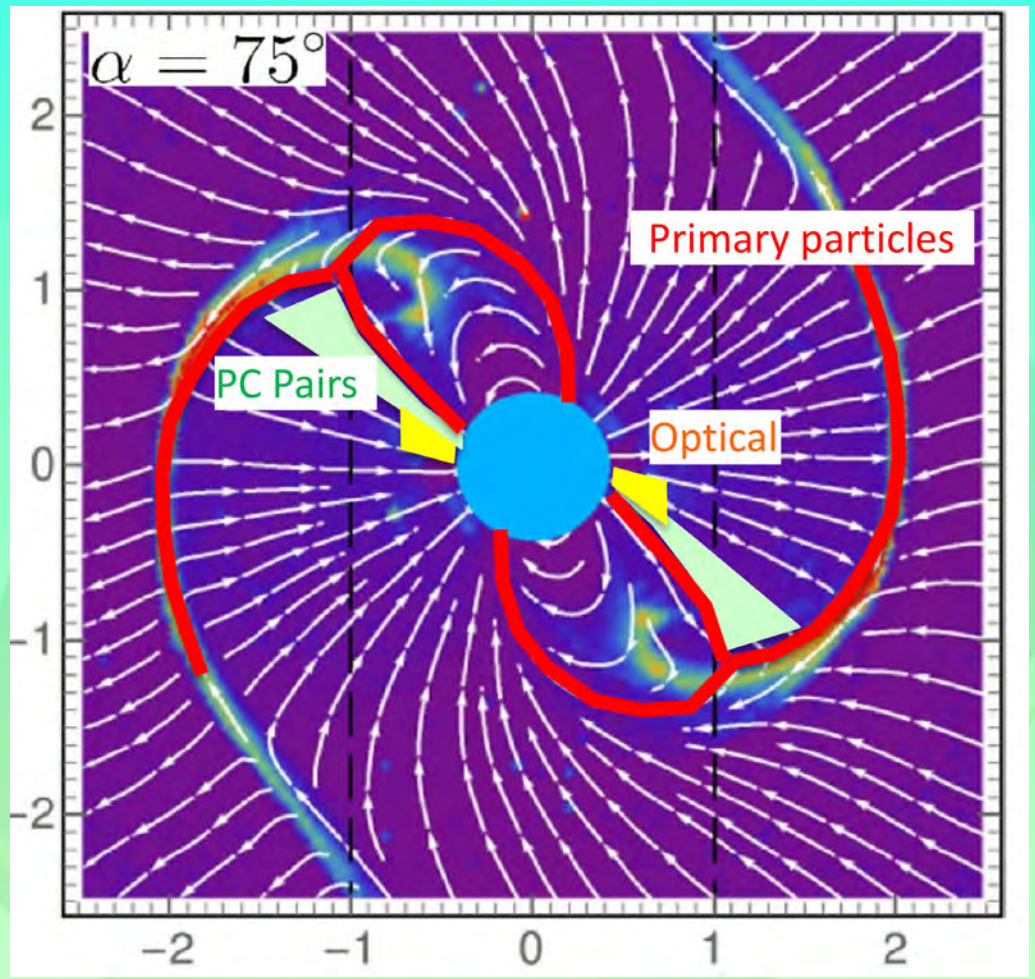

Harding & Kalapotharakos 2015
Harding et al. 2018
Harding et al. 2021

VHE pulsed emission (TeV+)

5+2 parameters: $E_{||}^{low}$, $E_{||}^{high}$, M_{+}, r_{radio}, J/J_{GJ} + α, ζ

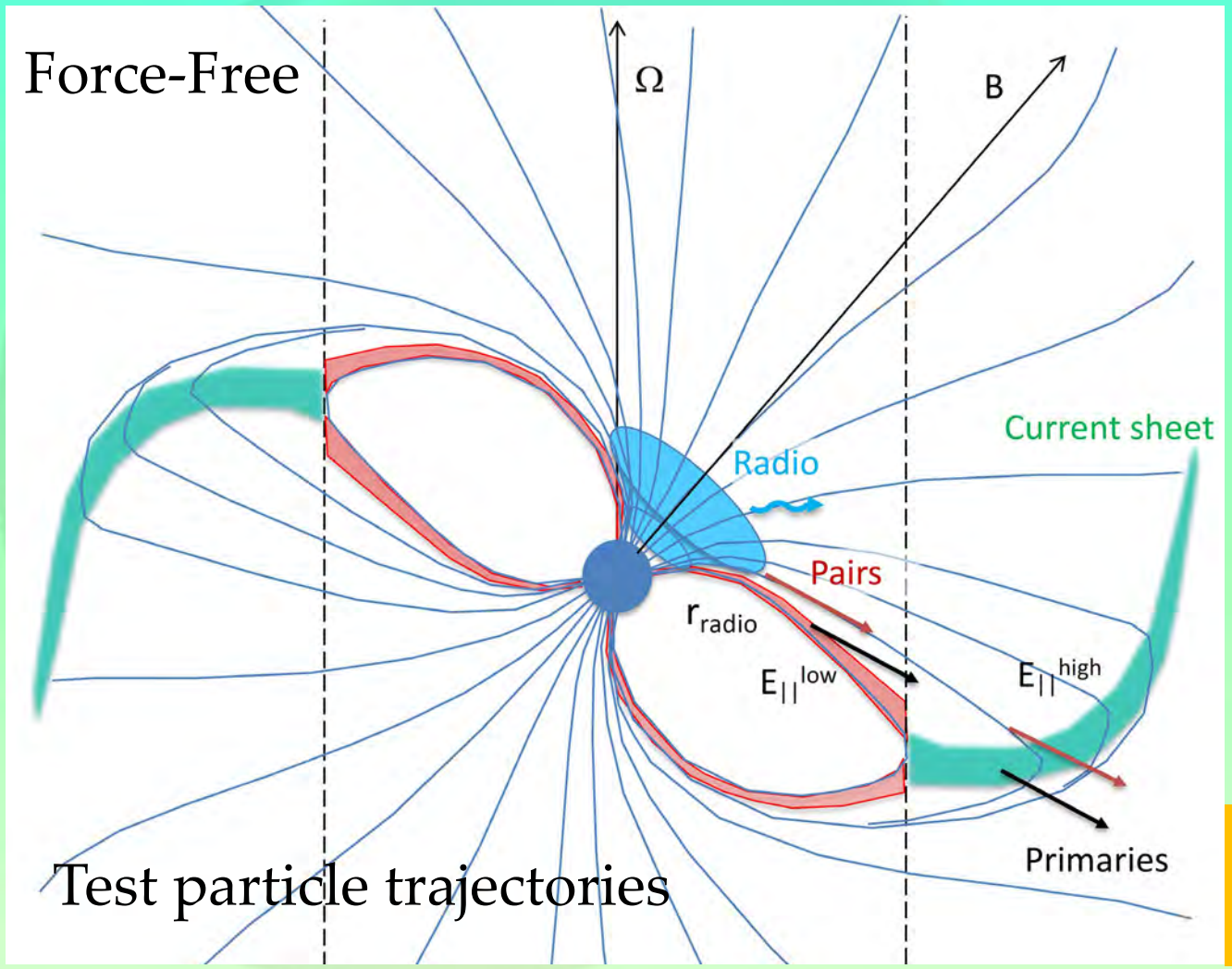

Pairs get pitch angles through resonant absorption of radio photons

Petrova & Lybarski 1998

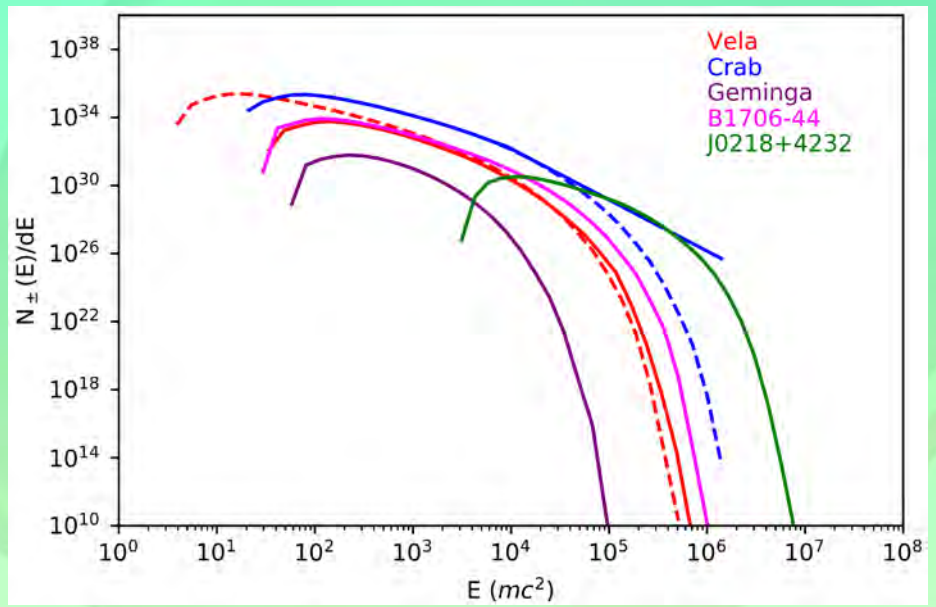

Harding & Kalapotharakos 2015
Harding et al. 2018
Harding et al. 2021

VHE pulsed emission (TeV+)

Vela

5+2 parameters: $E_{||}^{\text{low}}$, $E_{||}^{\text{high}}$, M_+, r_{radio}, J/J_{GJ} + α, ζ

Pairs: synchrotron radiation optical/UV at lower altitude

Primary particles (mostly e^+): synchro-curvature, peak at multi-GeV, up to 100 GeV in the curvature radiation regime

Primary particles (mostly e^+): scatter optical/UV photons to produce ~10TeV ICS emission

Pairs: scatter optical/UV photons to produce synchro-self-Compton 1-10 GeV for young and ~100 GeV for millisecond pulsars

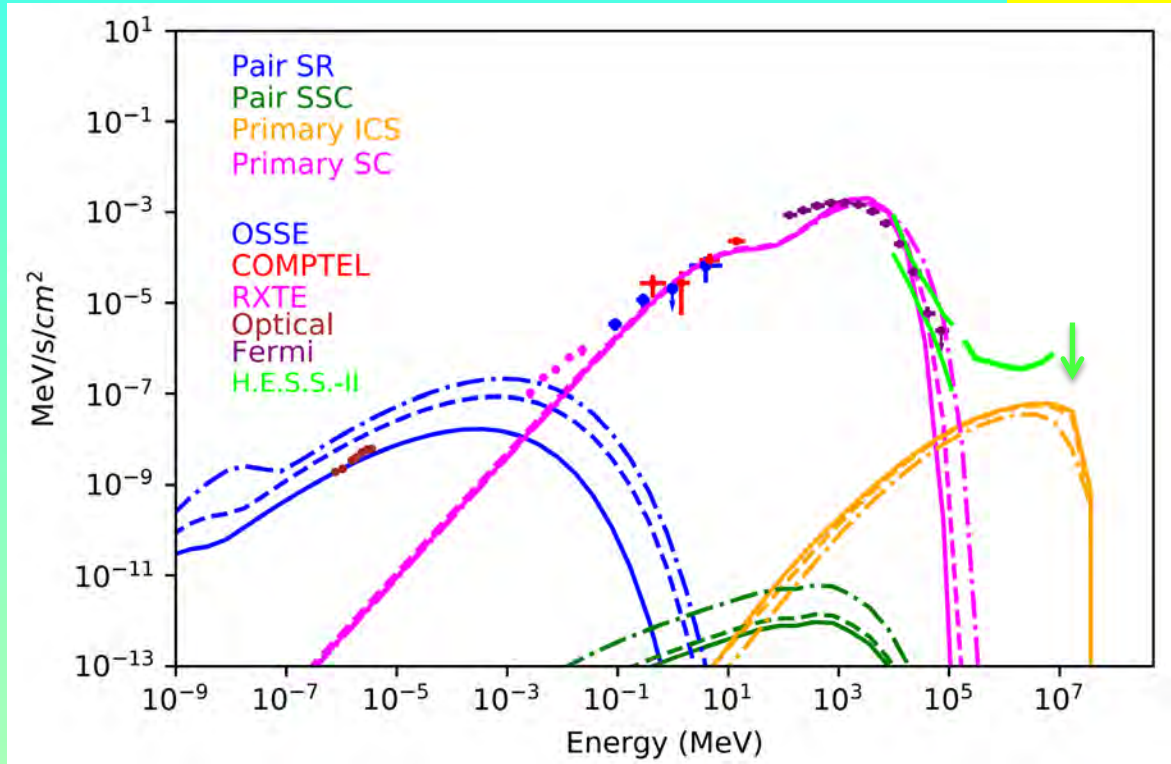

Broadband spectrum

Harding & Kalapotharakos 2015
Harding et al. 2018
Harding et al. 2021

VHE pulsed emission (TeV+)

Geminga

5+2 parameters: $E_{||}^{\text{low}}$, $E_{||}^{\text{high}}$, M_+, r_{radio}, J/J_{GJ} + α, ζ

Pairs: synchrotron radiation optical/UV at lower altitude

Primary particles (mostly e^+): synchro-curvature, peak at multi-GeV, up to 100 GeV in the curvature radiation regime

Primary particles (mostly e^+): scatter optical/UV photons to produce ~10TeV ICS emission

Pairs: scatter optical/UV photons to produce synchro-self-Compton 1-10 GeV for young and ~100 GeV for millisecond pulsars

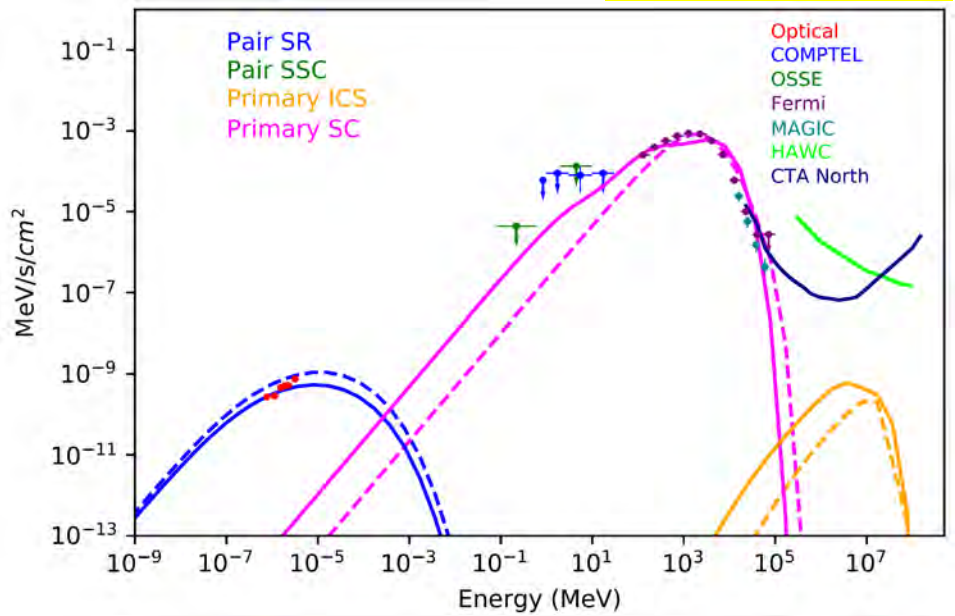

B1706-44

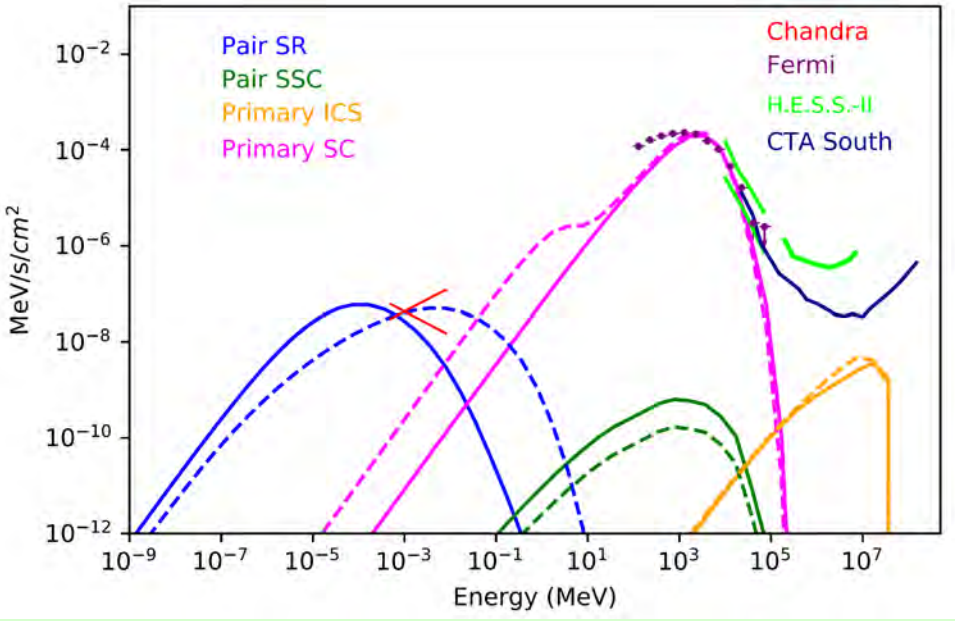

VHE pulsed emission (TeV+)

Crab

5+2 parameters: $E_{||}^{\text{low}}$, $E_{||}^{\text{high}}$, M_+, r_{radio}, J/J_{GJ} + α, ζ

Pairs: synchrotron radiation optical/UV at lower altitude

Primary particles (mostly e^+): synchro-curvature, peak at multi-GeV, up to 100 GeV in the curvature radiation regime

Primary particles (mostly e^+): scatter optical/UV photons to produce ~10TeV ICS emission

Pairs: scatter optical/UV photons to produce synchro-self-Compton 1-10 GeV for young and ~100 GeV for millisecond pulsars

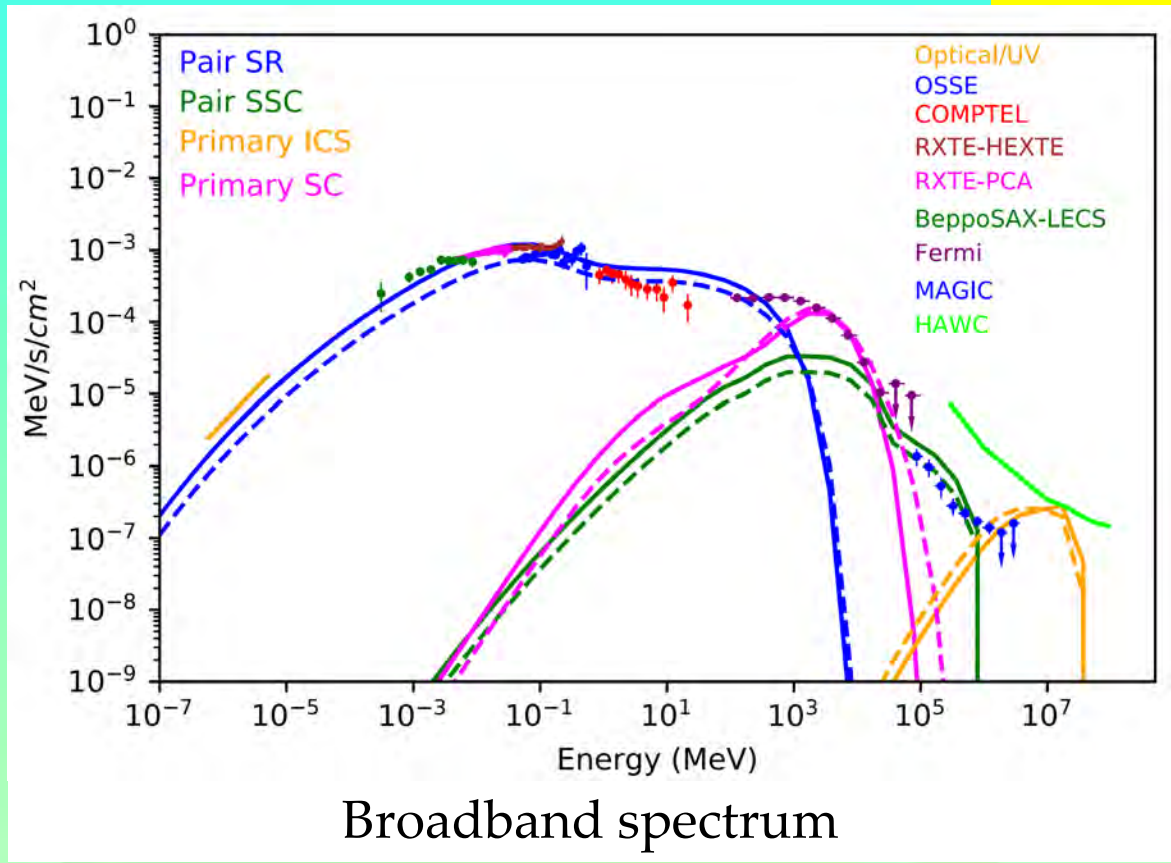

Broadband spectrum

Harding & Kalapotharakos 2015
Harding et al. 2018
Harding et al. 2021

VHE pulsed emission (TeV+)

Vela

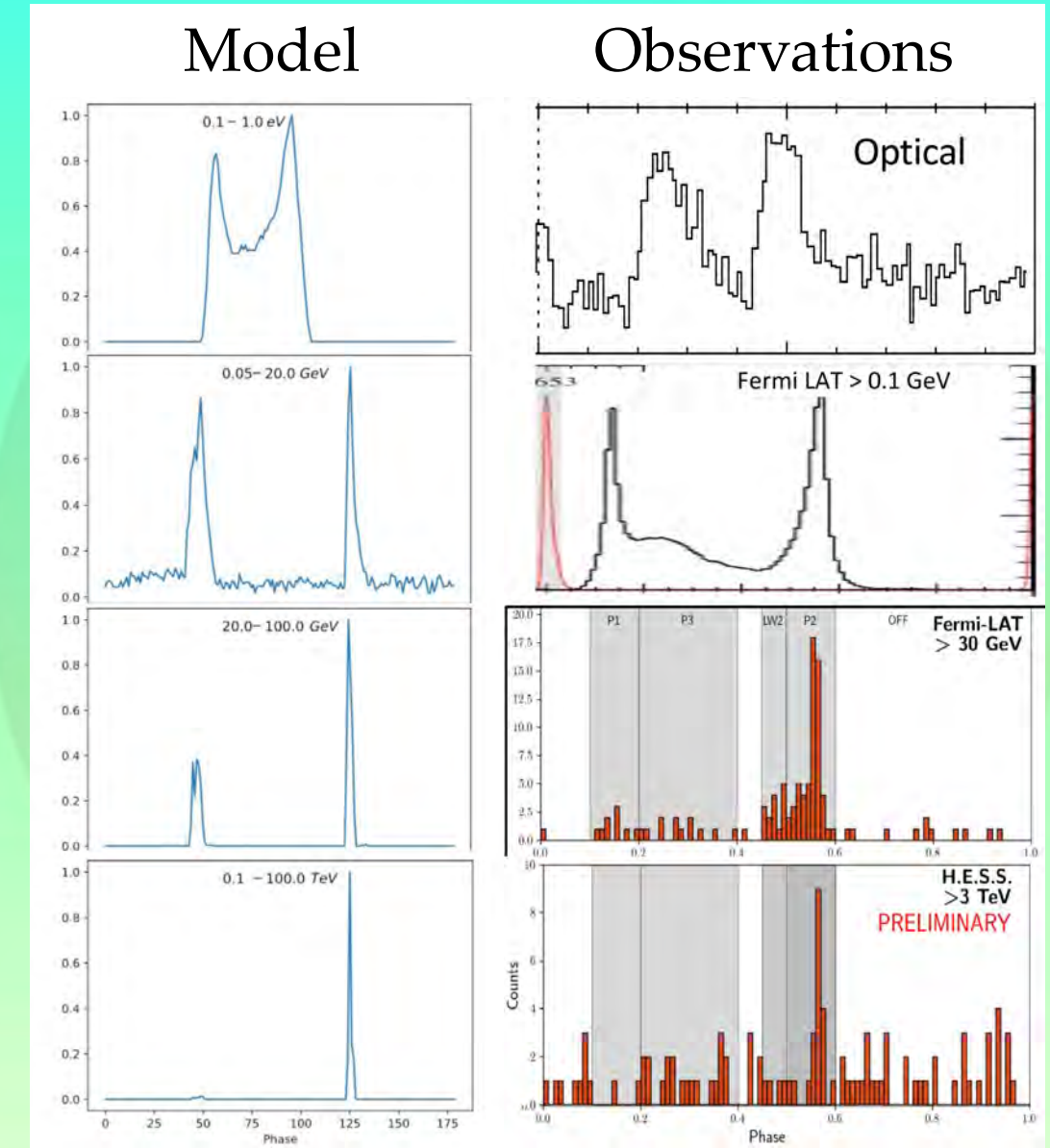

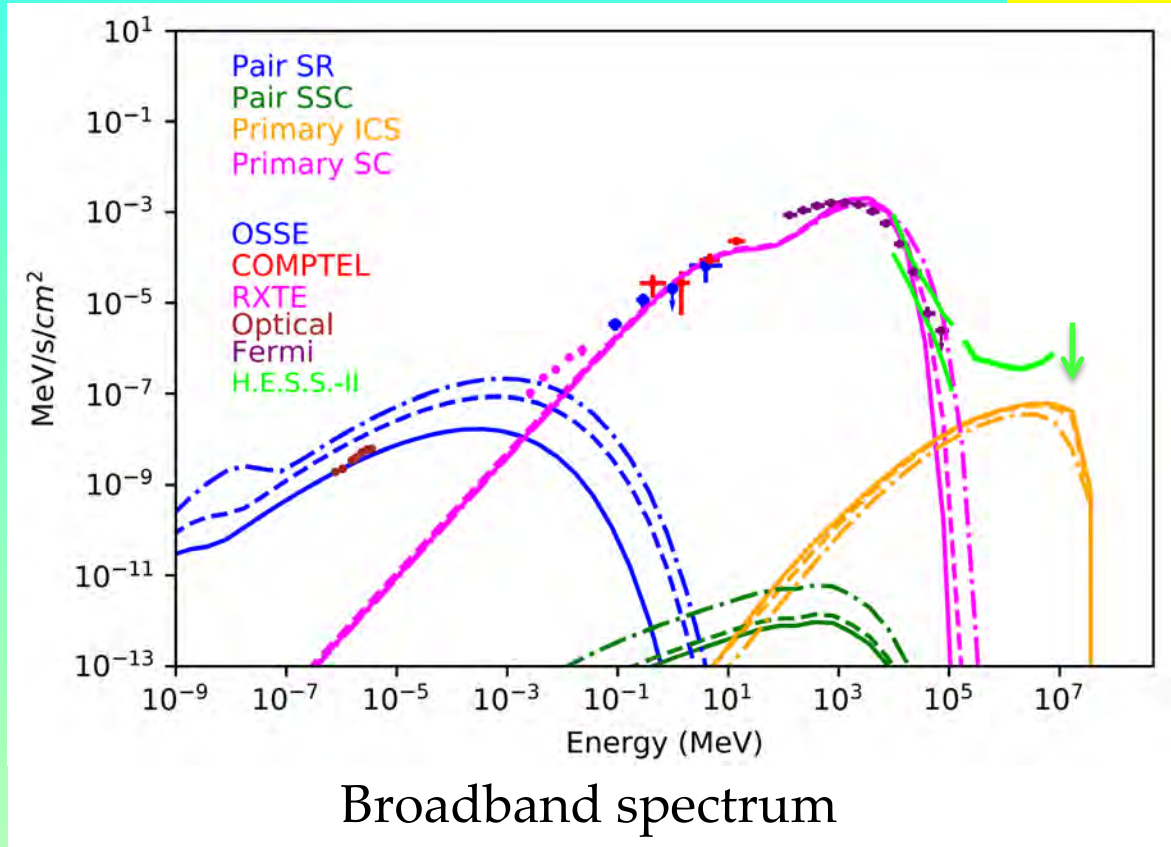

Broadband spectrum

Harding & Kalapotharakos 2015
Harding et al. 2018
Harding et al. 2021

VHE pulsed emission (TeV+)

Vela

Pulsed emission ~10 TeV requires particles energies > 10 TeV (ICS)

↓

Consistent with curvature radiation (instead of synchrotron) and the **FP theory**

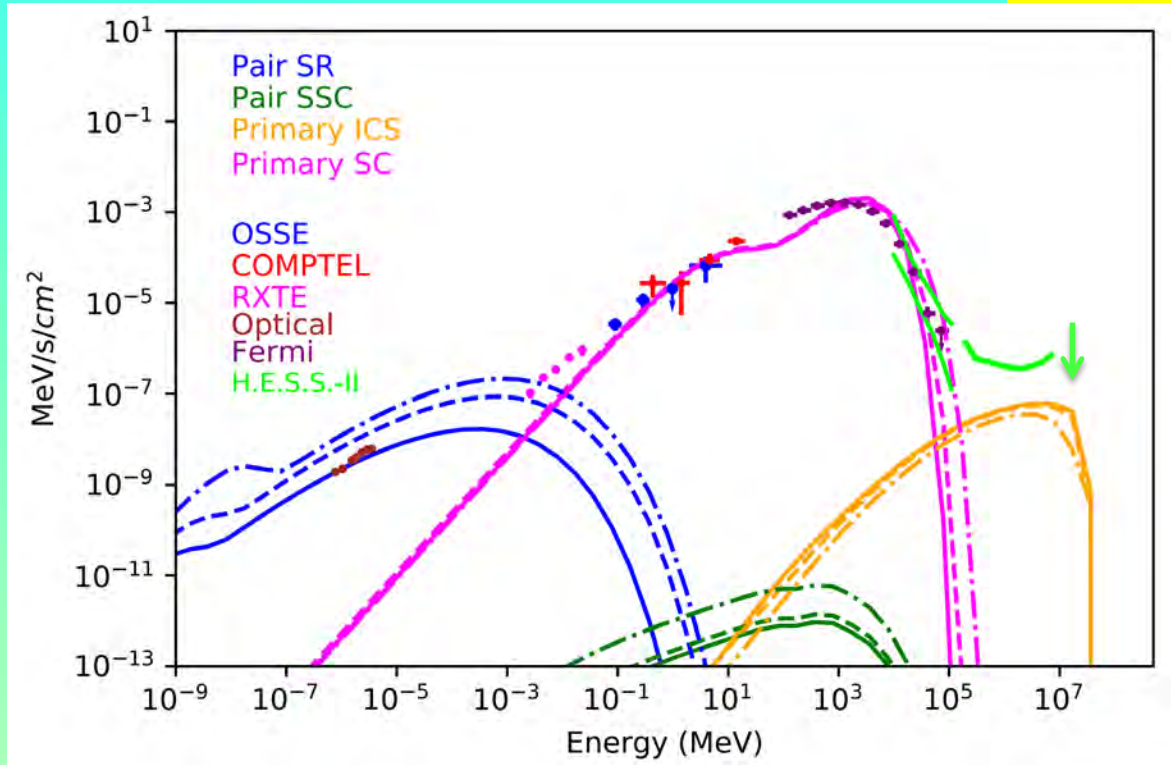

Broadband spectrum

Harding & Kalapotharakos 2015
Harding et al. 2018
Harding et al. 2021

Summary

Thank you very much!

Fundamental Plane of Gamma-Ray Pulsars

Relation between $L_\gamma, \dot{\mathcal{E}}, \varepsilon_{cut}, B_*$

$L_\gamma \propto \epsilon_{cut}^{1.18\pm0.24} B_*^{0.17\pm0.05} \dot{\mathcal{E}}^{0.41\pm0.08}$ **Fermi data**

$L_\gamma \propto \epsilon_{cut}^{4/3} B_*^{1/6} \dot{\mathcal{E}}^{5/12}$ **Theory CR**

Broadband and VHE emission models

The TeV emission is produced by ICS when high-energy primary particles scatter the low-energy photons.

The high-energy particles that are required are consistent with curvature radiation and the FP theory.

Kinetic PIC Models: Separatrix injection model Reproduce the γ-ray light curve patterns (δ-Δ) and the fundamental plane.

Models vs. Fermi data:

Deep understanding and a first-principle description of the entire population of γ-ray pulsars.

Death lines: Imply a new era of MeV pulsars (?)